Journal of Affective Disorders 372 (2025) 287–295

Contents lists available at ScienceDirect

Journal of Affective Disorders

journal homepage: www.elsevier.com/locate/jad

Research paper

Frontal localisation of a theory-based anxiety disorder biomarker – Goal conflict specific rhythmicity

Shabah M. Shadli [a,e], Bruce R. Russell [b], Veema Lodhia [d], Ian J. Kirk [d], Paul Glue [c], Neil McNaughton [a,*]

[a] Dept. Psychology, New Zealand
[b] School of Pharmacy, New Zealand
[c] Dept. Psychological Medicine, University of Otago, Dunedin, New Zealand
[d] Dept. Psychology, University of Auckland, Auckland, New Zealand
[e] School of Psychology, Charles Sturt University, Bathurst, NSW, Australia

ARTICLE INFO

Keywords:
Anxiety
Biomarker
Source localisation
EEG

ABSTRACT

Purpose: Anxiety disorders are a major global issue. Diagnosis via symptoms, not biological causes, delivers poor treatment outcomes. Our frontal EEG biomarker, Goal Conflict Specific Rhythmicity (GCSR; 4–12 Hz), developed from our long-standing detailed neuropsychological theory of anxiety processes, is reduced by all chemical types of *selective* anxiolytic and is high in cases across a range of currently diagnosed anxiety disorders.
Methods: We assessed frontal sources of GCSR, recording scalp EEG at either low resolution (Experiment 1, 32 channels, University of Otago, ♀:33, ♂:16) or high resolution (Experiment 2, 128 channels, University of Auckland, ♀:10, ♂:8) in healthy participants performing a Stop Signal Task to generate GCSR as previously.
Principal results: sLORETA demonstrated GCSR sources consistently in the right inferior frontal gyrus and, more strongly but less consistently, medial frontal gyrus. Variation was consistent with that of stopping in the same Stop Signal Task, depending on task demands.
Major conclusions: The sources of GCSR are consistent with our theory that hippocampal output receives goal information, detects conflict, and returns a negative biasing signal to the areas encoding goals in the current task. They match the variation in the control of stopping when response urgency changes. GCSR appears to index a biological type of anxiety unlike any current diagnosis and should help improve accuracy of diagnosis – anchored to actions of selective anxiolytic drugs. This task-related frontal "theta" rhythmicity provides proof-of-concept for further development of our theory of the neuropsychology of anxiety in direct human tests.

1. Introduction[1]

Anxiety disorders are currently the most prevalent psychiatric diseases in Europe and the USA (Kessler et al., 2005; Kessler et al., 2012), and the sixth highest cause of years of life lived with disability (Baxter et al., 2014). In 2010, 7 % of all suicide mortality globally was estimated to be attributable to anxiety disorders (Baxter et al., 2014). They are a grave and ever-increasing burden on healthcare resources (Cryan and Sweeney, 2011; Kessler, 2007; Maron and Nutt, 2017). COVID-19 increases psychiatric morbidity (Taquet et al., 2021) and vice versa (Wang et al., 2021); in a potential vicious cycle. Anxiety disorders also tend to start early in life (Cryan and Sweeney, 2011; Maron and Nutt, 2017) and often result in chronic impairment (Meyer, 2017).

Weak and inconsistent definitions of 'anxiety' (McNaughton, 2018) and inadequate psychiatric diagnosis (Insel, 2013) are key problems. Psychiatric diagnostic systems are regularly updated (Griebel and Holmes, 2013) but they use lists of signs and symptoms (American Psychiatric Association, 2013; World Health Organisation, 2010) not

* Corresponding author at: Department of Psychology, University of Otago, PO Box 56, Dunedin 9054, New Zealand.
E-mail address: neil.mcnaughton@otago.ac.nz (N. McNaughton).

[1] The content of this paper overlaps the preliminary report of the same data in the PhD thesis of the first author Shadli, S.M., 2014. An improved human anxiety-specific biomarker: frequency band, modality specificity, personality, pharmacology, and source characterisation. Department of Psychology. University of Otago, Dunedin. A preprint has been posted on Research Square, DOI: 10.21203/rs.3.rs-4844743/v1.*Abbreviations:* avPFC = anteroventral prefrontal cortex; DLPFC = dorsolateral prefrontal cortex; GCSR = Goal Conflict Specific Rhythmicity; MFG = medial frontal gyrus; rIFG = right inferior frontal gyrus; preSMA = pre-supplementary motor area; SSD = stop signal delay; SSRT = stop signal reaction time.

https://doi.org/10.1016/j.jad.2024.12.007
Received 25 August 2024; Received in revised form 7 November 2024; Accepted 1 December 2024
Available online 5 December 2024

fundamental underlying biological mechanisms of dysfunction (Insel et al., 2010). This is the equivalent of diagnosing COVID from its most common symptoms of fever, chills, and a sore throat rather than from a rapid antigen test detecting the biological cause: SARS-CoV-2 virus. So, anxiety treatment is poorly targeted (Scult et al., 2017), creating high costs and societal impact (Maron and Nutt, 2017).

We have a long-standing detailed preclinical neuropsychological theory (Gray and McNaughton, 2000; McNaughton and Corr, 2004; McNaughton and Gray, 2024) of the evolutionarily-conserved neural systems (McNaughton, 1990, 1999; Okamoto and Aizawa, 2013) that are adapted for survival in the face of threat (LeDoux, 2012). A unique feature of our theory is that it uses selective anxiolytic drugs (discussed further below) to define a specific biological form of anxiety and link it to its underlying neural systems. This has resulted in both distinct psychological definitions of anxiety and fear and what, until recently (see Bannerman et al., 2004, for review), was an unconventional view of the septo-hippocampal system as central to anxiety. In our theory, a 'fear' system controls reactions adapted for defensive ***avoidance*** and an 'anxiety' system (the Behavioural Inhibition System/Goal Inhibition System) controls reactions adapted for cautious defensive ***approach*** – resolving approach-avoidance conflicts (McNaughton and Corr, 2004).

Unlike other theories, then, we see fear and anxiety as almost opposites. This distinction derives from our unique pharmacological approach, where the 'anxiety' system is affected (and *defined)* by drugs acting at benzodiazepine or $5HT_{1A}$ receptors (Gray and McNaughton, 2000); the 'fear' system is not, but reacts to panicolytics, e.g., specific serotonin reuptake inhibitors (SSRI). Careful consideration of the common effects of selective anxiolytic drugs and septo-hippocampal lesions led to our emphasis on goal conflict as a core feature of anxiety (Gray and McNaughton, 2000; McNaughton and Gray, 2024). Note that definitional elasticity has resulted in DSM-5 (American Psychiatric Association, 2013) including fear/phobias within "anxiety" disorders. Also, importantly, anxiety disorder resulting from hyperactivity of the systems defined by selective anxiolytics, as a class, would require novel diagnosis and would only partially overlap a range of current DSM-5 diagnoses. A key goal of our current research is to identify a neural means of providing such a novel diagnosis.

One key finding for the theory is that all selective anxiolytic drugs reduce low frequency (theta and alpha range) hippocampal rhythmicity (see McNaughton et al., 2007, for review). This appears to provide a causal basis for the similarity of the behavioural effects of anxiolytics to those of septo-hippocampal lesions via changes in the processing of goal conflict (Gray and McNaughton, 2000; McNaughton and Gray, 2024). Septo-hippocampal rhythmicity could therefore provide a biomarker for a process fundamental to anxiety processing at the state level and the basis for one form of anxiety disorder at the trait level. However, depth recording in neurologically healthy humans is not feasible and scalp EEG recording cannot pick up signals from as deep a structure as the hippocampus. Fortunately, we have shown in rats that hippocampal rhythmicity linked to risk assessment (a core anxiety-linked behaviour) is coupled to synchronous rhythmicity in frontal cortex (Young and McNaughton, 2009). The theory, therefore, predicts that goal conflict should produce low frequency rhythmicity in frontal areas that is sensitive to selective anxiolytic drugs.

Goal conflict, and so behavioural inhibition, is held to occur when approach and avoidance are equally strong (Gray and McNaughton, 2000; McNaughton and Gray, 2024). Neo and McNaughton (2011) held $ gain constant and increased $ loss over 3 levels and compared the frontal EEG response across trials with net gain, balanced gain and loss (conflict), and net loss. At the right frontal site (F8) conflict produced greater 4-7 Hz (theta) rhythmicity than either gain or loss. This result was produced with participants recruited from Student Job Search who value the small monetary payments (typically totalling only a few dollars over an entire session). But a problem for clinical translation is that the typical patient is unlikely to react in the same way. We therefore turned to a task where motivation is intrinsic.

Stopping is a key element of behavioural inhibition. Right frontal cortex is thought to control simple, fast, stopping as produced in the Stop Signal Task (Aron et al., 2004, 2014). Importantly, the stopping and going processes are thought to be independent, resulting in a kind of horse race (Logan et al., 1984). So, in this task, we can vary the stop signal delay (SSD) from a value where stopping is easy (short SSD), to a value where stopping is difficult and so going occurs instead (long SSD). With medium SSDs, stopping occurs ~50 % of the time. In terms of our goal conflict theory of anxiety (Gray and McNaughton, 2000; McNaughton and Gray, 2024) conflict should be low with both short and long SSDs where negative and positive motivation predominate, respectively. Importantly, conflict should be high (and anxiolytic-sensitive) with medium SSDs when there is a balance between strong negative and strong positive motivation.

Based on this analysis, we have recently developed (McNaughton et al., 2013; Neo et al., 2011; Shadli et al., 2015) a human anxiety-specific right-frontal (F8) EEG biomarker in the Stop Signal Task (SST). To obtain this we measure 4-12 Hz power for each of short, medium, and long SSDs. We average the power for the low-conflict short and long SSDs to remove effects of variables that change steadily during the SSD interval and then subtract the result from the high-conflict medium SSD value. We also subtract the equivalent periods from matching go trials to retain only pure effects of the stop signal. The remainder of these subtractions is Goal Conflict Specific Rhythmicity (GCSR) that, within our theory, should be a biomarker for anxiety as we have defined it.

Importantly, given the definition of goal conflict within our theory, GCSR is sensitive to all three classes of *selective* anxiolytic drug (i.e. GABA-A, 5HT-1A, and calcium channel agents; McNaughton et al., 2013; Shadli et al., 2015). That is, drugs that improve some cases of generalized anxiety and social anxiety but not both major depression and panic disorder, nor PTSD or OCD (see Table 1 in McNaughton and Glue, 2020). GCSR is high in some cases across a range of conventional DSM "anxiety disorder" diagnoses (Shadli et al., 2021a) but not all cases within any current specific DSM diagnosis. It therefore appears to be a biomarker for a particular biological type of anxiety disorder that does not map directly to any of the current symptom-based ones. Similarly, while GCSR generally increases as trait anxiety scale scores increase, being particularly strong when trait anxiety is at clinical levels, it varies across diagnoses (generalized anxiety, generalized anxiety with co-morbid depression, social anxiety, other) despite these diagnostic groups not differing in terms of their conventional trait anxiety scores (Shadli et al., 2021a).

Our detailed theory, particularly its most recent edition, sees selective anxiolytic drugs as ultimately affecting subcortical and prefrontal structures (McNaughton and Gray, 2024, see Chapter 11 on prefrontal cortex). The selective anxiolytics act directly on areas such as the medial supramammillary nucleus to alter the "theta" (5–12 Hz) rhythmicity of hippocampal processing (McNaughton et al., 2006; Woodnorth and McNaughton, 1999, 2002). This, in turn, alters iterative integration (McNaughton and Vann, 2022) of goal representations in prefrontal cortex (McNaughton and Bannerman, 2024). But, we have not yet determined which frontal areas GCSR activates – our current proposal (Neo et al., 2011) is that, in the SST, conflict involves a circuit through some part of anteroventral prefrontal cortex that is in parallel to the fast and slow circuits controlling stopping (Fig. 1). Identifying the frontal sources of GCSR would allow it to be more firmly linked to the detailed neurology of the theory from which it was conceptually developed.

Consistent with Fig. 1, stopping ability is impaired by lesions in rIFG (Aron et al., 2003; Aron et al., 2004). Also, lesions in preSMA and SMA impaired stopping in the SST when responding was quicker (Floden and Stuss, 2006). Neuroimaging (fMRI) has also identified several neural networks activated during stopping of an already initiated response – involving rIFG, dorsolateral prefrontal cortex (DLPFC, areas 91, 101 and 46), medial frontal gyrus (MFG, areas 8 m and 9 m), basal ganglia (Aron, 2011; Aron et al., 2007; Aron et al., 2014; Chambers et al., 2009; Li et al.,

Table 1
Demographic data for the source localisation experiments.

	Age	M/F	EPQ			BIS	STAI-T	GO_RT	SSRT	$P_{inhibit}$ %		
			Neur	Extr	Psy					Short	Medium	Long
Low resolution EEG	21	31/14	11	14	6	13	30	441	223	70	51	10
B1								426	230	67	41	7
B3								465	217	75	47	12
High resolution EEG	20	8/10	13	11	5	11	32	479	224	76	47	8
B1								489	234	71	42	9
B3								460	216	78	47	8

Notes: M/F = Number of male and female participants per group; GO_RT = reaction time on Go trials in ms; SSRT = stop signal reaction time (Mean SSD on the intermediate staircase subtracted from median Go reaction time); $P_{inhibit}$ = Probability of inhibition on STOP trails; Neur = EPQ-R Neuroticism; Extr = EPQ-R Extraversion, Psy = EPQ-R Psychoticism, STAI-T = STAI-Trait; BIS = Behavioural Inhibition scale. B1, B3 data for Block 1 and Block 3 only – other data for all three blocks to match prior reports.

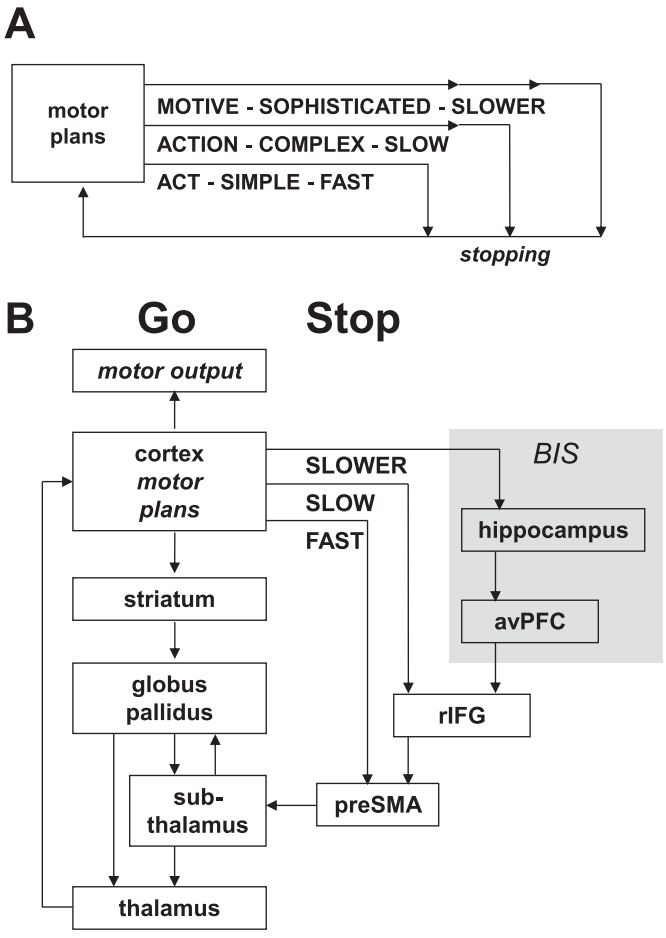

Fig. 1. Postulated neural control of going and stopping. A: general organisation of motor plans for stopping. Different types of response output, determined by required speed of response, engage different circuits. B: Neural pathways involved in going and stopping in the SST. Motor inhibition uses both fast and slow routes (Nachev et al., 2008a) to modulate the Go circuit (Nachev et al., 2005; Nachev et al., 2007a). For the fastest stopping preSMA and this output bypasses rIFG acting as a 'kill-switch' type of inhibitory control (Floden and Stuss, 2006). We proposed (Neo et al., 2011) that goal inhibition involves, in addition, the Behavioural Inhibition System (BIS, Gray and McNaughton, 2000). avPFC = anteroventral prefrontal cortex; rIFG = right inferior frontal gyrus; preSMA = pre-supplementary motor area. Connections have been simplified and circuits and structures in the BEHAVIOURAL INHIBITION SYSTEM, other than the hippocampus, are not shown (e.g., the Papez circuit is omitted). From Neo et al. (2011) with permission of the authors.

2006; Rubia et al., 2003; Verbruggen and Logan, 2008) and superior frontal gyrus (SFG; Rae et al., 2015).

Based on this existing evidence, we predicted that the estimated source of EEG activity related to GCSR would also be in the rIFG, with the possibility of additional involvement of DLPFC, MFG, and SFG. Based on the speculative 'avPC' in Fig. 1, we also expected activity in some area, rostral to rIFG, that would be relaying hippocampal output. (There is no direct hippocampal input to rIFG, McNaughton and Gray, 2024, Fig. 11.2A.)

However, we were prepared for some variation from this simple picture. In relation to our rIFG/MFG predictions, our one previous sLORETA EEG study of GCSR using a more complex selective stopping task found variations in frequency, drug-sensitivity, and the extent of involvement of rIFG and/or MFG across bilateral, selective ipsi-, and selective contra-lateral stopping (Shadli et al., 2020a). Likewise, testing left- versus right-handed participants, we found at F7/F8 *both* ipsi- and contra-lateral activation in *both* groups – with right-sided activation (F8) in right handers being mirrored by left-sided activation (F7) in left handers (Shadli et al., 2021c).

Here we first carried out an sLORETA assessment of our previously collected low-density (32 channel) data at the University of Otago; obtaining a coarse estimate of GCSR localisation with relatively large $N = 49$. Next, for replication and generalisation, we carried out an sLORETA at the School of Psychology, University of Auckland, using their high density 128 channel EEG system. This has better spatial resolution and source localisation (Michel et al., 2004; Tucker, 1993). This provided high resolution but with relatively low $N = 18$.

2. Method and materials

2.1. Participants

Participants reported themselves free of past psychological disorders and as right-handed. We restricted recruitment to right-handers because as discussed in the introduction previous experiments had GCSR most consistently at the right frontal site F8 (see also Shadli et al., 2021c). All participants gave their signed informed consent prior to participation in their respective experiments. Specific demographic details are given with each experiment.

There were 49 participants aged between 18 and 25 years (33 female, 16 male) in the low-density sLORETA experiment. Of these, we excluded 4 participants' data because of noisy EEG data. They were originally recruited from Otago University through advertisements via the organisation Student Job Search for an analysis of the relationship of personality to GCSR (Shadli et al., 2015) and subsequently re-analysed with sLORETA. They each received $20 reimbursement for participating but no financial incentives or disincentives in the task. The experimental and recruitment procedures were approved by the University of Otago Ethics Committee (approval number: DP 10/07).

There were 18 participants aged between 18 and 25 years (10 female, 8 male) in the high density sLORETA experiment. They were recruited to provide a replication and generalisation of the low-density results from University of Auckland through Departmental advertisement. Of these, we excluded 2 participants' data because they not fully complete the SST task. They were all reimbursed $20 in recognition of the inconvenience associated with the experiment but received no monetary reward or punishment during the task. This experiment was approved by The University of Auckland Human Participants Ethics Committee (Approval No: 8969).

All the work described has been carried out in accordance with The Code of Ethics of the World Medical Association (Declaration of Helsinki) http://www.wma.net/en/30publications/10policies/b3/index.html.

2.2. Questionnaires

For the EEG experiments, the participants filled out the Eysenck Personality Questionnaire-revised (EPQ-R, Eysenck and Eysenck, 1991), the BIS/BAS scale (Carver and White, 1994) and the Spielberger State-Trait Anxiety Inventory (STAI; Spielberger and Gorsuch, 1983), STAI-Trait questionnaire and then the STAI-State questionnaire before doing the SST task. Then, they performed the SST followed by another STAI-State questionnaire.

2.3. EEG recording – low density

For the low-density experiment, recording methods were as previously reported for a different analysis of a subset of the same participants.

> "Participants were fitted with an appropriately-sized Waveguard EEG cap (ANT Neurotechnology. Netherlands) with Ag/AgCl electrodes. Recordings taken from 34 channels of the extended International 10:20 system: Fp1, FpZ, Fp2, GND, F7, F3, Fz, F4, F8, FC5, FC1, FC2, FC6, T7, C3, Cz, C4, T8, CP5, CP1, CPz, CP2, CP6, P7, P3, Pz, P4, P8, POz, O1, Oz, O2, M1 and M2 (mastoids). CPz was used as the recording reference and data were re-referenced to the average of M1 and M2 during processing. A 3ml syringe and Precision Glide 16-gauge blunt needle (Becton, Dickenson & Co, New Jersey, USA) was used to insert Electro-gel (Electro Cap International, USA) into each of the 34 electrodes. The cap was connected to an ASA Neurotechnology EEG machine (eego, ANT Neurotechnology, Netherlands) and impedance adjusted to below 10 KΩ. [The sampling rate was 128 Hz], during export for processing, a filter was set to band pass 1-36 Hz. All participants underwent recording in a certified body protected room (i.e., with all power delivered through a residual-current circuit breaker) in the Department of Psychology at the University of Otago." (Shadli et al., 2021c, p. 213–214)

2.4. EEG recording – high density

For the high-density experiment, as described in a preliminary PhD thesis report, based on only 10 of the participants,

> "EEG recordings were performed in an electrically shielded room using 128 channel Ag/Agcl electrode nets (Electrical Geodesics Inc., Eugene, OR, USA) (Teyler et al., 2005). EEG was recorded continuously, sampling rate was 1000 Hz, and the analogue band pass was set to 0.1 to 400 Hz with Electrical Geodesics Inc. amplifiers (300-MΩ input impedance). The impedances were set below 40 KΩ, which is the standard for this system (Ferree et al., 2001). Cz was the reference electrode for this experiment (see re-referencing below). Vertical and horizontal electro-oculograms (VEOG and HEOG) were recorded and subsequently employed for artefact rejection. There were three different sizes of nets used for this experiment. We selected nets depending on the participant's head circumference. … When the participant finished filling out their questionnaire, we applied the net to their head very gently and then checked the impedance. If any electrode was above 30 KΩ, we applied some more solution underneath that electrode. They then started the SST task. They then filled out the STAI-state questionnaire." (Shadli, 2014, p. 96)

2.5. Stop signal task

As previously described in Shadli et al. (2021c, p. 214),

> "Visual Basic 6 code (suitable for use with EEG) for the SST is provided as [VB6 code 2015-10-16.zip] in Shadli et al. (2021b). The SST was based on Aron and Poldrack (2006) as modified by Shadli et al. (2015): short and long SSDs were set to a proportion of the participant's ongoing Go reaction time as in Carter et al. (2003) and medium SSDs tracked 50 % stopping by changing in relation to the participants' immediately preceding response. Note that only the medium SSD is the type of staircase used by Aron and Poldrack (2006) and is the only one that should be included in estimates of SST. The separate control of the short and long SSDs is designed to provide three distinct sets with equal numbers of trials to better estimate GCSR as detailed in Shadli et al. (2015). GCSR can be estimated from the standard SST procedure by splitting the obtained SSDs into three groups (McNaughton et al., 2013; Neo et al., 2011) but this delivers very different and statistically undesirable numbers across the trial types, with poor sampling of short and/or long SSDs.

Smiley and frowny faces provided 'successful' and 'unsuccessful' feedback, respectively. Instructions emphasised fast Go responding and, during SST blocks, if the participants went slow relative to their pre-training Go trial block (>1.5 x mean reaction time), 'SLOW!' was provided as feedback.

For 'Go' trials, a white fixation circle appeared at the center of the screen on a black background. 500 ms later, it was replaced by a green circle containing a left (<=) or right (=>) arrow, requiring a left or right mouse click, respectively. This prevented premature responding and a high percent correct indicated appropriate attention to the task. After this response, or following 1000 ms without a click, the fixation circle and arrow disappeared from the screen and ☺/☹/SLOW! feedback was presented as required. There was a 1000 ms inter-trial interval. 'Null events were imposed between every Stop or Go trial. The duration of null time ranged between 0.5 and 4 s (mean, 1 s; sampled from an exponential distribution truncated at 4 s)' as in Aron and Poldrack (2006, p. 2425).

Stop Trials started exactly like Go trials, but had a 1000 Hz auditory tone after a variable length SSD from arrow presentation that signalled the participant not to click. The tone stopped on a click or after 500 ms with no click. Before commencing the task, participants were told that both the Go trials and Stop trials were of equal importance. They were also told that the programme was designed such that they might not be able to get each of their click responses correctly. The successful, unsuccessful, and slow feedback were the same in Stop trials.

There were three blocks of 99 Go trials and 33 Stop trials with rest breaks between blocks, with one Stop trial within each 4 Go trials, counterbalanced. Stop trials were of three types: short SSD, medium SSD, and long SSD – in counterbalanced order. At the start of each block, participants were presented with the same set of instructions."

For further details and a schematic of the events in the task see Shadli et al. (2015); both code for the task and a SetUp package are available from Mendeley Data (Shadli et al., 2021b).

2.6. SSD control

The SSD control procedure was specially developed to produce an

improved GCSR as described at the beginning of the SST section. Participants' short SSDs were set to 20 %, and long SSDs to 70 %, of their Go reaction time averaged over the previous 16 Go trials. Medium SSDs were set at the beginning of a block to 45 % of the average Go reaction time for the last 16 trials of the previous block; and then increased (making stopping more difficult) when participants withheld responding correctly and decreased (making stopping easier) when participants responded incorrectly, forming a "staircase" of values as in Aron and Poldrack (2006) but with a 30 ms tracking step rather than 50 ms and a minimum of 50 ms gap between it and the current value of the short and long SSDs.

2.7. 2.6 EEG data analysis

For high and low resolution sLORETA, after finishing data collection, EEG files were segmented with their respective event markers into 750-ms epochs (including a 250-ms pre-stimulus baseline). Trials with eye blinks or eye movements artefacts were rejected. Power was averaged in the range 4–12 Hz. Source localization was performed using low-resolution electro-magnetic tomography (sLORETA) (Pascual-Marqui, 2002) employing all 32 (low resolution) or 129 (high resolution) channels. The sLORETA/eLORETA software package uses a non-parametric methodology. "It is based on estimating, via randomization, the empirical probability distribution for the max-statistic (e.g. the maximum of a t or an F statistic), under the null hypothesis. This methodology corrects for multiple testing (i.e., for the collection of tests performed for all electrodes and/or voxels, and for all time samples and/or discrete frequencies [(see Nichols and Holmes, 2002 for a complete overview of the methodology and how it properly corrects for multiple testing)]" (https://www.uzh.ch/keyinst/NewLORETA/Methods/MethodsSnPMloreta.htm). We used an in-house program to segment data for both stop and matching Go trials. We sorted the segmented files into short, medium and long groups for both stop and Go trials (i.e., 6 separate types of file). Then we made two separate folders for each of Go trials (A1, A2) and stop trials (B1, B2) and put medium SSD trials into "1" and short *and* long SSD trials into "2". We used the standard sLORETA statistics, independent group test, to test if A1-A2 = B1-B2. Note that, in effect, the subtraction represents a quadratic contrast of SSD (−1, +2, −1) while the equality test has the effect of a Stop-Go contrast. The result is a single value representing the linear (Stop-Go) × quadratic (SSD) contrast as would be calculated by a conventional SPSS repeated measures ANOVA.

3. Results

3.1. Demographic results

Table 1 shows the demographics for the two experiments: the overall mean Go reaction time was between 441 and 489 ms and the stop signal reaction time (SSRT) was between 223 and 234 ms. The average percentage of inhibition for short, medium and long delays were 67–78 %, 42–51 % and 8–12 % respectively. Note that both correct and incorrect stop trials were included in the EEG analysis with approximately the same number of trials for each SSD type.

3.2. Low resolution sLORETA

As shown in Fig. 2, the anatomical sources (averaged across participants and thresholded at $p < 0.05$) of the difference of average of short and long SSDs from medium SSD in power between stop and matching Go trials at 4–12 Hz frequency in Block-1 were strongest in the medial frontal gyrus (yellow pixels) with weaker activity in the rIFG (white elipse). In Block-3 the strongest activity was in the rIFG region (yellow pixels).

3.3. High resolution sLORETA

As shown in Fig. 3, the anatomical sources (averaged across

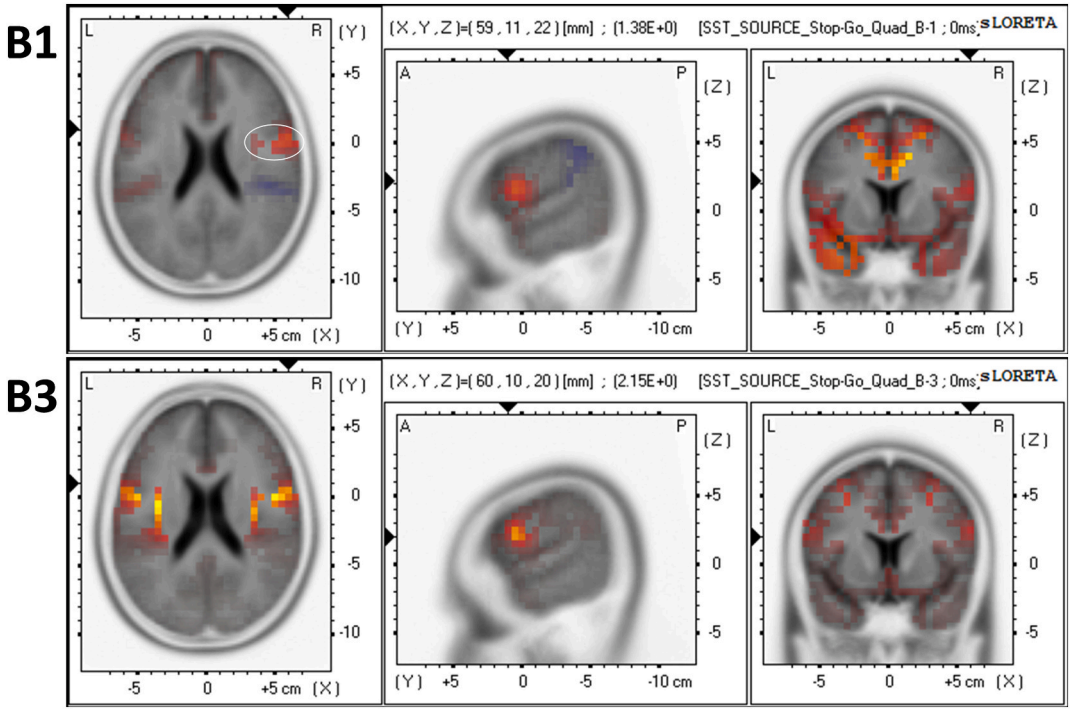

Fig. 2. Low density (32 channel) sLORETA. Axial slices of the brain showing the anatomical locations of GCSR activation (assessed as the significant difference of average of short and long SSDs from medium SSD (in EEG at source) between stop and adjacent Go trials at the time point at which stop signals were delivered in the stop trials). The upper figure shows the activation in Block-1 and the lower figure shows the activation in Block-3 of the SST. L = Left hemisphere; R = right hemisphere; x, y, z: coordinates of maximum activated voxel in standard MNI152 space; white ellipse encloses a weak rIFG activation.

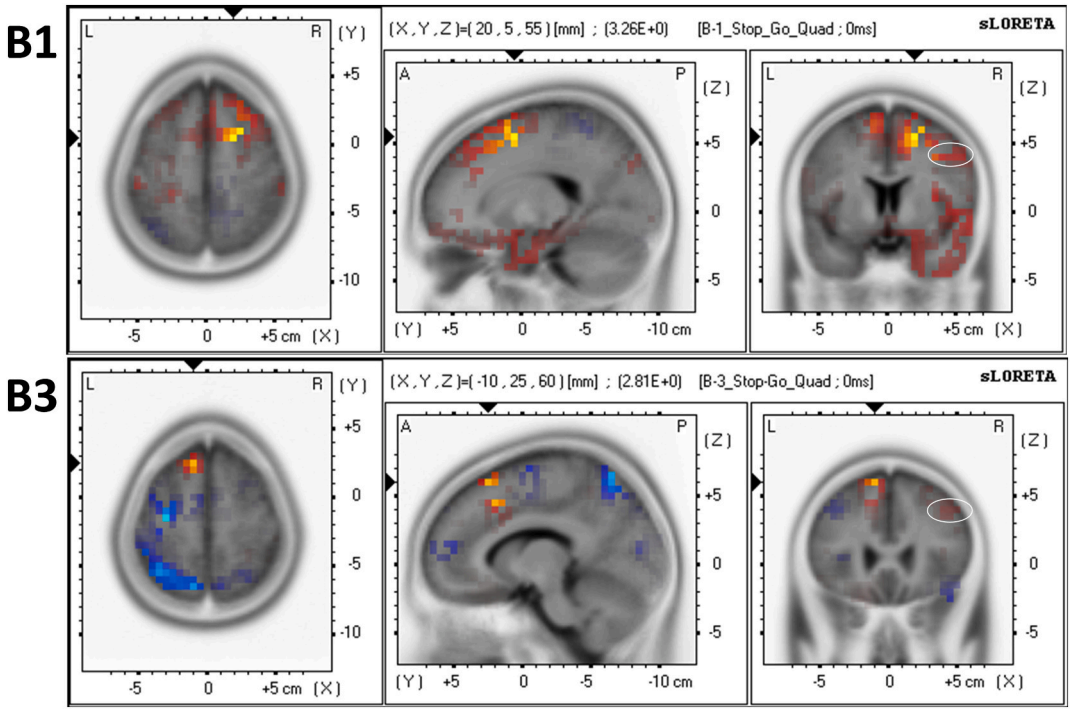

Fig. 3. High density (129 channel) sLORETA. Axial slices of the brain showing the anatomical locations of GCSR activation (assessed as the significant difference of average of short and long SSDs from medium SSD (in EEG at source) between stop and adjacent Go trials at the time point at which stop signals were delivered in the stop trials). The upper figure shows the activation in Block-1 and the lower figure shows the activation in Block-3 of the SST, where there was also deactivation (blue pixels). L = Left hemisphere; R = right hemisphere; X, Y, Z: coordinates of maximum activated voxel in standard MNI152 space; white ellipses enclose weak rIFG activations. (For interpretation of the references to color in this figure legend, the reader is referred to the web version of this article.)

participants and thresholded at $p < 0.05$) of the difference of average of short and long SSDs from medium SSD in power between stop and matching Go trials at 4–12 Hz frequency in Block-1 were the medial frontal gyrus (yellow pixels) of the frontal lobe and also, less so the rIFG (white elipse); and in Block-3 were the left superior frontal gyrus (yellow pixels) and, very weakly, the rIFG (white elipse). The activation of rIFG in both blocks of SST was consistent with our earlier broad band GCSR at F8.

4. Discussion

We predicted that the estimated source of EEG activity related to GCSR would be in rIFG, and possibly DLPFC, MFG, and SFG. As shown in Table 2, all these areas showed at least some activity in at least some cases. The area most *consistently*, but not always strongly, activated is rIFG, followed by rMFG. For both IFG and MFG when left-side activation occurred it was concurrent with right (see also Shadli et al., 2021c). In contrast, in one case left DLPFC shows GCSR but right does not. We also speculated that there would be activity in some area ('avPC' in Fig. 1) rostral to rIFG that would be relaying hippocampal output. We did not

Table 2
Summary of significant Goal Conflict Specific Rhythmic activations seen in key frontal structures across a range of experiments.

Expt.	Paradigm	EEG	R-IFG	R-MFG	L-IFG	L-MFG	R-DLPFC	L-DLPFC	SSRT
2	SST B3	High							216
1	SST B3	Low							217
1	SST B1	Low							230
2	SST B1	High							234
*	SS	Low							224
*	SG	Low							370
*	GS	Low							526

Notes: * (Shadli et al., 2020a); 1–2 as reported above. Paradigm includes stop condition for the selective stopping task (SG = stop left only; SS = stop both; GS = stop right only) and block for the stop signal task. Results are ranked by mean SSRT for SST and selective stopping, separately. Method identifies sLORETA as low/high depending on resolution (32/128 channels). Previously defined sites of interest are identified as R/L for right/left with IFG = inferior frontal gyrus, MFG = medial frontal gyrus, DLPFC = dorsolateral prefrontal cortex. Additional single site results are reported in the text. Yellow = high activation; Brown = moderate activation; Salmon = weak/restricted activation.

clearly identify such an area.

Our data are consistent with evidence for at least two different neural networks that can generate stopping in the SST: involving rIFG (Aron et al., 2003; Aron et al., 2014; Verbruggen and Logan, 2008) and MFG (Johansen-Berg et al., 2004; Nachev et al., 2008b; Nachev et al., 2007b), respectively. We also found a GCSR source in the SFG, consistent with fMRI studies of stopping (Rae et al., 2015). During executing stopping action, there is evidence of activations of multiple neural networks using direct, indirect and hyper-direct pathways (Nambua et al., 2002; Rae et al., 2015; Wiecki and Frank, 2013). Our results suggest that goal conflict can interact with all of the areas that control stopping.

As with stopping control itself, the location of GCSR appears to depend on the time pressure of stopping and the resultant strategies chosen by participants. For both tasks, a longer SSRT produced greater GCSR activation of rIFG and, less clearly, shorter SSRT was more likely to involve MFG. Stopping was faster in block 1 than block 3 for both SST experiments – probably because participants respond faster at the start of the SST using a strategy developed during the initial pure-Go training phase and later slowing their responses strategically in an attempt to achieve more accurate stopping. This would be consistent with the suggestion of Floden and Stuss (2006, p 1847) "that both superior medial and lateral regions of the right frontal lobe appear to participate in response inhibition depending on task requirements"; with GCSR activation following a similar pattern.

Fig. 1 outlines our starting hypothesis (Neo et al., 2011) that the Behavioural Inhibition System (Gray and McNaughton, 2000) – recently renamed the Goal Inhibition System (McNaughton, 2020; McNaughton and Gray, 2024) to avoid confusion with some personality scale constructs – is an additional outer, particularly slow, layer of the neural control of stopping that involves goals rather than the action and act stopping described by Aron et al. (2003) and Floden and Stuss (2006), respectively. In our BEHAVIOURAL/GOAL INHIBITION SYSTEM theory, the hippocampus can continuously receive goal information (and generate "theta" rhythm) in 'just checking' mode and only produces "theta"-paced output when it detects conflict. Its output would then impact on whichever areas had provided the initial input and these would vary from task to task and from response strategy to response strategy.

A key point, that follows from this target variability, is that the hippocampal-mediated action of selective anxiolytic drugs would be an alteration of the negative emotional bias of engrams in the target areas. On this view, at least some types of anxiety disorder would be the result of excessive formation of negative memories as a result of hippocampal biasing. The drugs would then block this biasing allowing the negative memories to extinguish over time. Consistent with this, treatment-sensitive DSM generalized anxiety disorder has high positive GCSR, while treatment-resistant DSM generalized anxiety disorder has negative GCSR (Shadli et al., 2024). Such a mechanism would account for the slow amelioration of anxiety proper when treated with selective anxiolytics.

"The novel anxiolytics require at least 10 days' administration to produce their therapeutic effect; so are generally seen to differ markedly from the apparently immediate benzodiazepines. This apparent immediacy likely explains the preference for benzodiazepines (Trimble, 1990) that remains among some clinicians to this day (Ait-Daoud et al., 2018). But on the Hamilton Anxiety Rating Scale, benzodiazepines take as long as novel anxiolytics to produce their effects (e.g., Wheatley, 1990, Fig. 14.2) and even with pre-operative anxiety, which might have been expected to be especially susceptible to acute anxiolytic effects, the benzodiazepines do not act immediately (Wikinski et al., 1994). The benzodiazepines appear to have two separate effects: 1) immediate euphoria and muscle relaxation (which show rapid tolerance); and 2) a slower truly anxiolytic effect (which does not show tolerance) that appears as the muscle relaxation and euphoria fade." (McNaughton and Gray, 2024, p. 89)

This difference between benzodiazepines and serotonergic agents is likely to be due to the fact that the former block the release of stress hormones, while the latter release them. When corticosterone levels are controlled, the anxiolytic actions of these two types of drug become similar (McNaughton et al., 1996). This suggests a mutual antagonism between endogenous stress hormones and endogenous anxiolytic hormones.

The current results lend support to the theory that at least one type of anxiety disorder results from negative cognitive bias produced by interaction of hippocampal hyperactivity with the storage of goal-related information in other parts of the brain (McNaughton, 1997). They also suggest that recording of GCSR from appropriate cortical areas in a suitably designed task could act as a clinical biomarker for such a disorder. However, it should be noted that the SST is not suitable for clinical use except on a single-use group basis (e.g., Shadli et al., 2021a; Shadli et al., 2024). It appears to lack sufficient sensitivity at the individual level and, critically, is unstable. It can give different results across blocks and can be eliminated by a prior relaxation test (Shadli et al., 2020b).

Development of more suitable goal-conflict tasks is needed. Conflict between reward and a virtual predator in a simple escape task is known to produce hippocampal and medial prefrontal activation that is related to trait anxiety (Fung et al., 2019); and we have preliminary evidence that a simplified version of this task generates GCSR across a range of frontal channels somewhat similar to those of the SST. However, its use of small monetary rewards and money-hungry students to generate conflict makes it unsuitable for the clinic. A more promising approach is the use of two-way avoidance (where conflict is between two different sources of threat). This allows control of levels of motivation that the SST does not. But a current version using the Joystick Operated Runway Task has not been validated with buspirone, is not affected by citalopram (Perkins et al., 2009), and shows narrow benzodiazepine dose-sensitivity (Lippold et al., 2020). We have preliminary evidence that our simplified version of the escape task, substituting avoidance of a second predator for gain of reward, can produce GCSR but this remains to be drug validated. Future work is needed to generate a measure suitable for clinical use.

A limitation, as for prior work with stopping-control circuits, is that variation in circuits involved in conflict-control remains a speculation. Also, given the variability of EEG, larger N would be preferable; as would combining EEG with concurrent fMRI (serial testing is contra-indicated, Shadli et al., 2020b); and manipulating strategic slowing. Our results are generally consistent with the proposed neurology both of stopping and of goal inhibition in the Stop Signal Task (McNaughton et al., 2013; Neo et al., 2011; Shadli et al., 2021a; Shadli et al., 2015).

5. Conclusion

Here, we have shown that sources of GCSR are consistent with the theory (Gray and McNaughton, 2000; McNaughton and Corr, 2004; McNaughton and Gray, 2024) that hippocampal output receives goal information, detects conflict, and returns a negative biasing signal to the areas encoding goals in the current task. Specifically, GCSR occurs in areas known to control stopping in the SST and its location varies in a way consistent with variation in the control of stopping when response urgency changes.

These results help to confirm the nature of a theoretically-based biological type of anxiety that is distinct from any current diagnosis. Such a biologically-based diagnosis should improve accuracy of diagnosis and, so, ultimately treatment. In particular, we hope to provide a novel, strong, biological definition of an anxiety disorder as defined by the action of selective anxiolytic drugs particularly on "theta" rhythm.

We would agree that the causal status of "theta" rhythmicity (i.e. 5–12 Hz) in any case of anxiety disorder remains to be determined. We see our work as a preliminary to developing a test of this. However, "theta" has been a reliable predictor of a drug's human clinical anxiolytic action for over 40 years (McNaughton and Sedgwick, 1978) with no

false positives or negatives (McNaughton et al., 2007); and its functional role in anxiolytic-sensitive behaviour has been demonstrated (McNaughton et al., 2006). Our results show that it is possible to record anxiolytic-sensitive rhythmicity in the hippocampal "theta" range of frequencies from task-related frontal sites with scalp recording.

Our results provided proof-of-concept for further development of our theory of the neuropsychology of anxiety in direct human tests. They also provide a spring-board for the development of more reliable biologically-based measures of anxiety processes and their use to define novel anxiety diagnoses.

CRediT authorship contribution statement

Shabah M. Shadli: Writing – original draft, Visualization, Project administration, Investigation, Formal analysis. **Bruce R. Russell:** Resources, Investigation, Funding acquisition, Formal analysis. **Veema Lodhia:** Investigation. **Ian J. Kirk:** Investigation. **Paul Glue:** Conceptualization. **Neil McNaughton:** Writing – review & editing, Writing – original draft, Visualization, Resources, Project administration, Methodology, Funding acquisition, Conceptualization.

Declaration of competing interest

Dr. Glue has a contract with Douglas Pharmaceuticals to develop novel ketamine formulations. No other authors have disclosures. No authors have conflicts of interest to declare.

Acknowledgements

This work was supported by the Health Research Council of New Zealand [Grant # 19/027].

Data availability

The data are available from Shabah Shadli <sshadli@csu.edu.au> on reasonable request.

References

Ait-Daoud, N., Hamby, A.S., Sharma, S., Blevins, D., 2018. A review of alprazolam use, misuse, and withdrawal. J. Addict. Med. 12, 4–10. https://doi.org/10.1097/ADM.0000000000000350.

American Psychiatric Association, 2013. Diagnostic and Statistical Manual of Mental Disorders, fifth edition. American Psychiatric Association, Arlington, VA.

Aron, A.R., 2011. From reactive to proactive and selective control: developing a richer model for stopping inappropriate responses. Biol. Psychiatry 69, e55–e68. https://doi.org/10.1016/j.biopsych.2010.07.024.

Aron, A.R., Poldrack, R.A., 2006. Cortical and subcortical contributions to stop signal response inhibition: role of the subthalamic nucleus. J. Neurosci. 26, 2424–2433. https://doi.org/10.1523/JNEUROSCI.4682-05.2006.

Aron, A.R., Fletcher, P.C., Bullmore, E.T., Sahakian, B.J., Robbins, T.W., 2003. Stop-signal inhibition disrupted by damage to right inferior frontal gyrus in humans. Nat. Neurosci. 6, 115–116. https://doi.org/10.1038/nn1003.

Aron, A.R., Robbins, T.W., Poldrack, R.A., 2004. Inhibition and the right inferior frontal cortex. Trends Cogn. Sci. 8, 170–177. https://doi.org/10.1016/j.tics.2004.02.010.

Aron, A.R., Behrens, T.E., Smith, S., Frank, M.J., Poldrack, R.A., 2007. Triangulating a cognitive control network using diffusion-weighted magnetic resonance imaging (MRI) and functional MRI. J. Neurosci. 27, 3743–3752. https://doi.org/10.1523/JNEUROSCI.0519-07.2007.

Aron, A.R., Robbins, T.W., Poldrack, R.A., 2014. Inhibition and the right inferior frontal cortex: one decade on. Trends Cogn. Sci. 18, 177–185. https://doi.org/10.1016/j.tics.2013.12.003.

Bannerman, D.M., Rawlins, J.N.P., McHugh, S.B., Deacon, R.M.J., Yee, B.K., Bast, T., Zhang, W.N., Pothuizen, H.H.J., Feldon, J., 2004. Regional dissociation within the hippocampus - memory and anxiety. Neurosci. Biobehav. Rev. 28, 273–283.

Baxter, A.J., Vos, T., Scott, K.M., Ferrari, A.J., Whiteford, H.A., 2014. The global burden of anxiety disorders in 2010. Psychol. Med. 44, 2363–2374. https://doi.org/10.1017/S0033291713003243.

Carter, D.J., Farrow, M., Silberstein, B.R., Stough, C., Tucker, A., Pipingas, A., 2003. Assessing inhibitory control: a revised approach to the stop signal task. J. Atten. Disord. 6, 153–161.

Carver, C.S., White, T.L., 1994. Behavioral inhibition, behavioral activation, and affective responses to impending reward and punishment: the BIS/BAS scales. J. Pers. Soc. Psychol. 67, 319.

Chambers, C.D., Garavan, H., Bellgrove, M.A., 2009. Insights into the neural basis of response inhibition from cognitive and clinical neuroscience. Neurosci. Biobehav. Rev. 33, 631–646. https://doi.org/10.1016/j.neubiorev.2008.08.016.

Cryan, J.F., Sweeney, F.F., 2011. The age of anxiety: role of animal models of anxiolytic action in drug discovery. Br. J. Pharmacol. 164. https://doi.org/10.1111/bph.2011.164.issue-4.

Eysenck, H.J., Eysenck, S.B.G., 1991. ADULT EPQ-R. Hodder Education, London.

Ferree, T.C., Luu, P., Russel, G.S., Tucker, D.M., 2001. Scalp electrode impedence, infection risk, and EEG data quality. Clin. Neurophysiol. 112, 536–544.

Floden, D., Stuss, D.T., 2006. Inhibitory control is slowed in patients with right superior medial frontal damage. J. Cogn. Neurosci. 18, 1843–1849.

Fung, B.J., Qi, S., Hassabis, D., Daw, N., Mobbs, D., 2019. Slow escape decisions are swayed by trait anxiety. Nat. Hum. Behav. 3, 702–708. https://doi.org/10.1038/s41562-019-0595-5.

Gray, J.A., McNaughton, N., 2000. The Neuropsychology of Anxiety: An Enquiry into the Functions of the Septo-Hippocampal System, 2 ed. Oxford University Press, Oxford.

Griebel, G., Holmes, A., 2013. 50 years of hurdles and hope in anxiolytic drug discovery. Nat. Rev. Drug Discov. 12, 667–687. https://doi.org/10.1038/nrd4075.

Insel, T., 2013. Transforming Diagnosis. National Institutes of Mental Health, NIMH Director's Blog.

Insel, T., Cuthbert, B., Garvey, M., Heinssen, R., Pine, D.S., Quinn, K., Sanislow, C., Wang, P., 2010. Research domain criteria (RDoC): toward a new classification framework for research on mental disorders. Am. J. Psychiatry 167, 748–751. https://doi.org/10.1176/appi.ajp.2010.09091379.

Johansen-Berg, H., Behrens, T.E., Robson, M.D., Drobnjak, I., Rushworth, M.F., Brady, J. M., Smith, S.M., Higham, D.J., Matthews, P.M., 2004. Changes in connectivity profiles define functionally distinct regions in human medial frontal cortex. Proc. Natl. Acad. Sci. U S A 101, 13335–13340. https://doi.org/10.1073/pnas.0403743101.

Kessler, R.C., 2007. The global burden of anxiety and mood disorders: putting ESEMeD findings into perspective. J. Clin. Psychiatry 68, 10–19.

Kessler, R.C., Chiu, W.T., Demler, O., Merikangas, K.R., Walters, E.E., 2005. Prevalence, severity, and comorbidity of 12-month DSM-IV disorders in the National Comorbidity Survey Replication. Arch. Gen. Psychiatry 62, 617–627. https://doi.org/10.1001/archpsyc.62.6.617.

Kessler, R.C., Petukhova, M., Sampson, N.A., Zaslavsky, A.M., Wittchen, H.U., 2012. Twelve-month and lifetime prevalence and lifetime morbid risk of anxiety and mood disorders in the United States. Int. J. Methods Psychiatr. Res. 21, 169–184. https://doi.org/10.1002/mpr.1359.

LeDoux, J., 2012. Rethinking the emotional brain. Neuron 73, 653–676. https://doi.org/10.1016/j.neuron.2012.02.004.

Li, C.S., Huang, C., Constable, R.T., Sinha, R., 2006. Imaging response inhibition in a stop-signal task: neural correlates independent of signal monitoring and post-response processing. J. Neurosci. 26, 186–192. https://doi.org/10.1523/JNEUROSCI.3741-05.2006.

Lippold, J.V., Ettinger, U., Hurlemann, R., Corr, P.J., Reuter, M., Perkins, A.M., 2020. Differentiating anxiety from fear: an experimental-pharmacological approach. Personal. Neurosci. 3, e6. https://doi.org/10.1017/pen.2020.1.

Logan, G.D., Cowan, W.B., Davis, K.A., 1984. On the ability to inhibit simple and choice reaction-time responses - a model and a method. J. Exp. Psychol. Hum. Percept. Perform. 10, 276–291.

Maron, E., Nutt, D., 2017. Biological markers of generalized anxiety disorder. Dialogues Clin. Neurosci. 19, 147–157.

McNaughton, N., 1990. Evolution and anxiety. In: McNaughton, N., Andrews, G. (Eds.), Anxiety. University of Otago Press, Dunedin, pp. 115–121.

McNaughton, N., 1997. Cognitive dysfunction resulting from hippocampal hyperactivity - a possible cause of anxiety disorder. Pharmacol. Biochem. Behav. 56, 603–611.

McNaughton, N., 1999. A gene promotes anxiety in mice - and also scientists. Nat. Med. 5, 1131–1132.

McNaughton, N., 2018. What do you mean "anxiety"? Developing the first anxiety syndrome biomarker. J. R. Soc. N. Z. 48, 177–190. https://doi.org/10.1080/03036758.2017.1358184.

McNaughton, N., 2020. Personality neuroscience and psychopathology: should we start with biology and look for neural-level factors? Personal. Neurosci. 3, e4. https://doi.org/10.1017/pen.2020.5.

McNaughton, N., Bannerman, D., 2024. The homogenous hippocampus: how hippocampal cells process goals. OSF Preprint. https://doi.org/10.31219/osf.io/a458n.

McNaughton, N., Corr, P.J., 2004. A two-dimensional neuropsychology of defense: fear/anxiety and defensive distance. Neurosci. Biobehav. Rev. 28, 285–305. https://doi.org/10.1016/j.neubiorev.2004.03.005.

McNaughton, N., Glue, P., 2020. Ketamine and neuroticism: a double-hit hypothesis of internalizing disorders. Personal. Neurosci. 3, e2. https://doi.org/10.1017/pen.2020.2.

McNaughton, N., Gray, J.A., 2024. The Neuropsychology of Anxiety: An Enquiry into the Functions of the Septo-Hippocampal System, 3 ed. Oxford University Press, Oxford.

McNaughton, N., Sedgwick, E.M., 1978. Reticular stimulation and hippocampal theta rhythm in rats: effects of drugs. Neuroscience 3, 629–632.

McNaughton, N., Vann, S.D., 2022. Construction of complex memories via parallel distributed cortical-subcortical iterative integration. Trends Neurosci. 45, 550–562. https://doi.org/10.1016/j.tins.2022.04.006.

McNaughton, N., Panickar, K.S., Logan, B., 1996. The pituitary-adrenal axis and the different behavioral effects of buspirone and chlordiazepoxide. Pharmacol. Biochem. Behav. 54, 51–56. https://doi.org/10.1016/0091-3057(95)02129-9.

McNaughton, N., Ruan, M., Woodnorth, M.A., 2006. Restoring theta-like rhythmicity in rats restores initial learning in the Morris water maze. Hippocampus 16, 1102–1110. https://doi.org/10.1002/hipo.20235.
McNaughton, N., Kocsis, B., Hajós, M., 2007. Elicited hippocampal theta rhythm: a screen for anxiolytic and procognitive drugs through changes in hippocampal function? Behav. Pharmacol. 18, 329–346. https://doi.org/10.1097/FBP.0b013e3282ee82e3.
McNaughton, N., Swart, C., Neo, P., Bates, V., Glue, P., 2013. Anti-anxiety drugs reduce conflict-specific "theta"—a possible human anxiety-specific biomarker. J. Affect. Disord. 148, 104–111. https://doi.org/10.1016/j.jad.2012.11.057.
Meyer, A., 2017. A biomarker of anxiety in children and adolescents: a review focusing on the error-related negativity (ERN) and anxiety across development. Dev. Cog. Neuro. 27, 58–68. https://doi.org/10.1016/j.dcn.2017.08.001.
Michel, C.M., Murray, M.M., Lantz, G., Gonzalez, S., Spinelli, L., Grave de Peralta, R., 2004. EEG source imaging. Clin. Neurophysiol.: official journal of the International Federation of Clinical Neurophysiology 115, 2195–2222. https://doi.org/10.1016/j.clinph.2004.06.001.
Nachev, P., Rees, G., Parton, A., Kennard, C., Husain, M., 2005. Volition and conflict in human medial frontal cortex. Curr. Biol. 15, 122–128. https://doi.org/10.1016/j.cub.2005.01.006.
Nachev, P., Wydell, H., O'Neill, K., Husain, M., Kennard, C., 2007a. The role of the pre-supplementary motor area in the control of action. Neuroimage 36, T155–T163. https://doi.org/10.1016/j.neuroimage.2007.03.034.
Nachev, P., Wydell, H., O'Neill, K., Husain, M., Kennard, C., 2007b. The role of the pre-supplementary motor area in the control of action. NeuroImage 36 (Suppl. 2), T155–T163. https://doi.org/10.1016/j.neuroimage.2007.03.034.
Nachev, P., Kennard, C., Husain, M., 2008a. Functional role of the supplementary and pre-supplementary motor areas. Nat. Rev. Neur. 9, 856–869. https://doi.org/10.1038/nrn2478.
Nachev, P., Kennard, C., Husain, M., 2008b. Functional role of the supplementary and pre-supplementary motor areas. Nat. Rev. Neurosci. 9, 856–869. https://doi.org/10.1038/nrn2478.
Nambua, A., Tokunob, H., Takada, M., 2002. Functional significance of the cortico-subthalamo-pallidal 'hyperdirect' pathway. Neurosci. Res. 43, 111–117.
Neo, P.S.H., McNaughton, N., 2011. Frontal theta power linked to neuroticism and avoidance. Cogn. Affect. Behav. Neurosci. 11, 396–403. https://doi.org/10.3758/s13415-011-0038-x.
Neo, P.S.H., Thurlow, J.K., McNaughton, N., 2011. Stopping, goal-conflict, trait anxiety and frontal rhythmic power in the stop-signal task. Cogn. Affect. Behav. Neurosci. 11, 485–493. https://doi.org/10.3758/s13415-011-0046-x.
Nichols, T.E., Holmes, A.P., 2002. Nonparametric permutation tests for functional neuroimaging: a primer with examples. Hum. Brain Mapp. 15, 1–25. https://doi.org/10.1002/hbm.1058.
Okamoto, H., Aizawa, H., 2013. Fear and anxiety regulation by conserved affective circuits. Neuron 78, 411–413.
Pascual-Marqui, R.D., 2002. Standardized low resolution brain electromagnetic tomography (sLORETA): technical details. Methods Find. Exp. Clin. Pharmacol. 24D, 5–12.
Perkins, A.M., Ettinger, U., Davis, R., Foster, R., Williams, S.C.R., Corr, P.J., 2009. Effects of lorazepam and citalopram on human defensive reactions: ethopharmacological differentiation of fear and anxiety. J. Neurosci. 29, 12617–12624. https://doi.org/10.1523/jneurosci.2696-09.2009.
Rae, C.L., Hughes, L.E., Anderson, M.C., Rowe, J.B., 2015. The prefrontal cortex achieves inhibitory control by facilitating subcortical motor pathway connectivity. J. Neurosci. 35, 786–794. https://doi.org/10.1523/JNEUROSCI.3093-13.2015.
Rubia, K., Smith, A.B., Brammer, M.J., Taylor, E., 2003. Right inferior prefrontal cortex mediates response inhibition while mesial prefrontal cortex is responsible for error detection. Neuroimage 20, 351–358. https://doi.org/10.1016/s1053-8119(03)00275-1.
Scult, M.A., Knodt, A.R., Radtke, S.R., Brigidi, B.D., Hariri, A.R., 2017. Prefrontal executive control rescues risk for anxiety associated with high threat and low reward brain function. Cereb. Cortex 1-7. https://doi.org/10.1093/cercor/bhx304.
Shadli, S.M., 2014. An Improved Human Anxiety-Specific Biomarker: Frequency Band, Modality Specificity, Personality, Pharmacology, and Source Characterisation. University of Otago, Dunedin, Department of Psychology.
Shadli, S.M., Glue, P., McIntosh, J., McNaughton, N., 2015. An improved human anxiety process biomarker: characterization of frequency band, personality and pharmacology. Transl. Psychiatry 5, e699. https://doi.org/10.1038/tp.2015.188.
Shadli, S.M., High, O., Byers, B., Gibbs, P., Steller, R., Glue, P., McNaughton, N., 2020a. Human anxiety-specific "theta" occurs with selective stopping and localizes to right inferior frontal gyrus. Behav. Neurosci. 134, 547–555. https://doi.org/10.1037/bne0000316.
Shadli, S.M., McIntosh, J., McNaughton, N., 2020b. Anxiety process "theta" biomarker in the stop signal task eliminated by a preceding relaxation test. Behav. Neurosci. 134, 556–561. https://doi.org/10.1037/bne0000328.
Shadli, S.M., Ando, L.C., McIntosh, J., Lodhia, V., Russell, B.R., Kirk, I.J., Glue, P., McNaughton, N., 2021a. Right frontal anxiolytic-sensitive EEG 'theta' rhythm in the stop-signal task is a theory-based anxiety disorder biomarker. Sci. Rep. 11, 19746. https://doi.org/10.1038/s41598-021-99374-x.
Shadli, S.M., Tewari, V., Holden, J., McNaughton, N., 2021b. GCSR_L-R-handers_2020-12-03. Mendeley Data V1. https://doi.org/10.17632/whc4p79vhm.1.
Shadli, S.M., Tewari, V., Holden, J., McNaughton, N., 2021c. Laterality of an EEG anxiety disorder biomarker largely follows handedness. Cortex 140, 210–221. https://doi.org/10.1016/j.cortex.2021.03.025.
Shadli, S.M., Donegan, C.J., Bin Mohd Fahmi, M.S., Russell, B.R., Glue, P., McNaughton, N., 2024. Is lack of goal-conflict-specific rhythmicity a biomarker for treatment resistance in generalised anxiety but not social anxiety or major depression? J. Psychopharmacol. https://doi.org/10.1177/02698811241275627, 2698811241275627.
Spielberger, C.D., Gorsuch, R., 1983. State-Trait Anxiety Inventory (Form Y). Consulting Psychologists Press.
Taquet, M., Geddes, J.R., Husain, M., Luciano, S., Harrison, P.J., 2021. 6-month neurological and psychiatric outcomes in 236 379 survivors of COVID-19: a retrospective cohort study using electronic health records. The Lancet Psychiatry, online. https://doi.org/10.1016/s2215-0366(21)00084-5.
Teyler, T.J., Hamm, J.P., Clapp, W.C., Johnson, B.W., Corballis, M.C., Kirk, I.J., 2005. Long-term potentiation of human visual evoked responses. Eur. J. Neurosci. 21, 2045–2050. https://doi.org/10.1111/j.1460-9568.2005.04007.x.
Trimble, M.R., 1990. Benzodiazepines in clinical practice. In: Wheatley, D. (Ed.), The Anxiolytic Jungle: Where Next. John Wiley & Sons, Chichester, pp. 9–21.
Tucker, T.M., 1993. Spatial sampling of head electrical fields: the geodesic sensor net. Electroencephalogr. Clin. Neurophysiol. 87, 154–163.
Verbruggen, F., Logan, G.D., 2008. Response inhibition in the stop-signal paradigm. Trends Cogn. Sci. 12, 418–424. https://doi.org/10.1016/j.tics.2008.07.005.
Wang, Q., Xu, R., Volkow, N.D., 2021. Increased risk of COVID-19 infection and mortality in people with mental disorders: analysis from electronic health records in the United States. World Psychiat. https://doi.org/10.1002/wps.20806 online first.
Wheatley, D., 1990. The new alternatives. In: Wheatley, D. (Ed.), In the Anxiolytic Jungle: Where Next? John Wiley, Chichester, pp. 163–184.
Wiecki, T.V., Frank, M.J., 2013. A computational model of inhibitory control in frontal cortex and basal ganglia. Psychol. Rev. 120, 329–355. https://doi.org/10.1037/a0031542.supp.
Wikinski, S., Lombardo, M., Medina, J.H., Rubio, M.C., 1994. Lack of anxiolytic effect of diazepam in pre-anaesthetic medication. Br. J. Anaesth. 72, 694–696.
Woodnorth, M.A., McNaughton, N., 1999. Anxiolytic action on the supramammillary nucleus reduces theta frequency and increases fixed interval responding. Soc. Neurosci. Abstracts 25, 1641.
Woodnorth, M.A., McNaughton, N., 2002. Benzodiazepine receptors in the medial-posterior hypothalamus mediate the reduction of hippocampal theta frequency by chlordiazepoxide. Brain Res. 954, 194–201.
World Health Organisation, 2010. International Statistical Classification of Diseases and Related Health Problems 10th Revision. http://apps.who.int/classifications/icd10/browse/2010/en.
Young, C.K., McNaughton, N., 2009. Coupling of theta oscillations between anterior and posterior midline cortex and with the hippocampus in freely behaving rats. Cereb. Cortex 19, 24–40. https://doi.org/10.1093/cercor/bhn055.